Experimental band structure of semimetal bismuth

G. Jezequel* and J. Thomas
Laboratoire de Spectroscopie du Solide (URA 1202 CNRS), Faculté des Sciences de l'Université de Rennes I, F-35042 Rennes-CEDEX, France

I. Pollini
Istituto Nazionale per la Fisica della Materia (INFM), Dipartimento di Fisica dell'Università di Milano, Via Celoria 16, 20133 Milano, Italy

(Received 9 April 1997)

Angle-resolved photoemission measured from the Bi(111) surface with synchrotron radiation between 7.5 and 100 eV exhibit strong features associated with valence-band states of p and s symmetry and electronic surface states. The valence-band dispersions of p and s states have been measured along the symmetry line $\Gamma\Lambda T$ of the Brillouin zone, which is mapped out by recording normal emission at 300 K and below 20 K, and by discussing the photoemission results in terms of the direct-transition model. The experimental bulk electronic structure is compared with the results of band-structure calculations, obtained by a pseudopotential approach (Golin) and a relativistic augmented-plane-wave (Ferreira) method. Finally, two narrow nondispersing peaks observed in the low-temperature photoemission spectra at binding energies 0.40 and 2.95 eV are assigned to surface (or resonance) states. [S0163-1829(97)07835-1]

I. INTRODUCTION

The electronic properties of Bi, like those of the group-V semimetals, such as As and Sb, have been for a long time the center of interest of many theoretical and experimental investigations. Bismuth is a prototype semimetal: its structure is noncubic and rather complicated; however, the packing density is comparable to that in metals.

Its interesting properties derive from the fact that a small effective number of carriers makes the charge transport, its Fermi surface is small and rather simple, relaxation times are long, and quantum effects relatively large. Most theoretical studies have concentrated on the carriers themselves, either studying the g factor of electrons[1] or their dispersion curves.[2,3] Detailed band-structure calculations were needed in order to study the effective masses,[4] the g factors,[5,6] the optical properties,[7] and the pressure effects.[8] A first tight-binding calculation made by Mase[9] correctly predicted the locations and symmetries of the carriers. Then, small but important regions of the Brillouin zone (BZ) near the symmetry points T and L, where the carriers are located, were studied by Abrikosov and Falkovski[10] and Falkovskii and Razina[11] with the same formalism.

In addition, the electronic band structure of bismuth has been studied by means of an empirical pseudopotential model (EPM) by Golin,[12] who obtained a good qualitative agreement with the effective masses of the carriers, and a quantitative agreement with the optical data. A relativistic augmented-plane-wave (APW) calculation made by Ferreira[13] introduced the relativistic corrections (mass velocity, Darwin, and spin orbit), which in the case of bismuth are quite large. The results for Bi compare well to those of As (Ref. 14) and Sb (Refs. 15–17) obtained by Falicov and co-workers, and scale regularly in the sequence As-Sb-Bi, forming a monotonic pattern. The only difference is the effect of the spin-orbit coupling over the Fermi surface, which in Bi becomes very different from that of Sb and As: in Bi, there is a crossover of bands along the ΓT direction, and a change of shape of the bands near the Fermi level (E_F).

X-ray photoelectron spectra of the valence bands of crystalline and amorphous bismuth have been measured[18] and compared with band-structure calculations; the values of binding energies of the valence s (10.36 and 11.54 eV) and p (1.30 and 3.45 eV) electrons and the average splitting between s and p bands (approximately 8.6 eV) have also been determined. The last value is comparable to the average s-p splitting in free atoms, which is about 9.7 eV. The binding energies of $5d_{3/2}$ and $5d_{5/2}$ core states are reported at 26.94 and 23.90 eV, respectively.

Theoretical band-structure calculations show indeed two well-separated s-like bands (Λ_6,Λ_6), several eV below the Fermi level (E_F) (between 9 and 13 eV) and three upper p-like bands ($\Lambda_6,\Lambda_{45},\Lambda_6$) near E_F (Refs. 9–15, and 17) (down to 2.85 eV).

Angle-resolved ultraviolet photoemission spectra (ARUPS) from the Bi(0001) surface have also been measured by diebowitz *et al.*,[19] with an instrumental resolution that allowed them to determine the occupied band structure with an accuracy of about 1 eV. The spectra only showed two broad features associated with valence bands of p symmetry, which were assigned to one-dimensional density of states. The semimetals As, Sb, and Bi all have the $A7$ (arsenic) crystal structure.[12,20] The unit cell is rhombohedral and contains two atoms. Having an even number of conduction electrons per primitive cell, they come very close to being insulators, but there is a slight band overlap leading to a very small number of carriers. Figure 1 shows the positions of the atoms in the structure: the trigonal axis is along the (111) direction. We can think of the $A7$ structure as being made by the proper stacking of the (111)-type atomic planes, in such a way that every six planes the structure repeats itself. It can be obtained from the simple cubic structure with

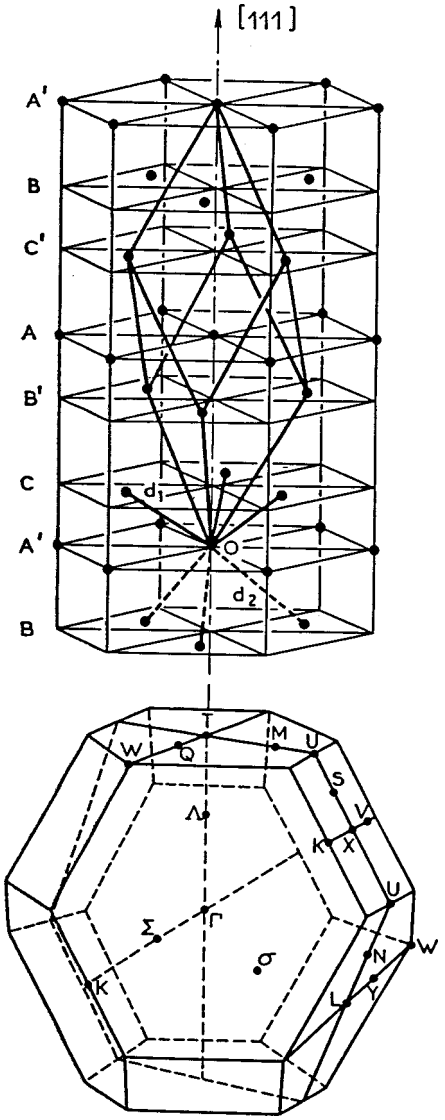

FIG. 1. Crystal structure of rhombohedral bismuth and its Brillouin zone showing points and lines of symmetry.

one atom at each lattice site by applying two independent distortions: a shear and an internal displacement of the atoms. The shear is along one body diagonal and transforms the unit cube into a rhombohedron. The diagonal retains the threefold symmetry and becomes the trigonal axis of the $A7$ structure. The main crystal structure parameters of bismuth at 4.2 K are the following: a_0 (lattice parameter) $=6.3081$ Å; α (rhombohedral angle) $=57°19'$, and u (internal displacement parameter) $=0.234\,07$.

The electronic level occupation in Bi is $5d^{10}6s^26p^3$: the $5d^{10}$ bands are occupied so that many-body problems in narrow partially filled bands are of no account and only $6s^2$ and $6p^3$states contribute to the occupied valence bands.

Because of partial filling of bands the electronic properties are those of a metal, but because of the smallness of the overlap a very small number of carriers (about 10^{-5} per atom) contribute to the conductivity. These low carrier densities explain why the pentavalent metals do not follow some typical predictions of the free-electron theory. Small pockets of carriers imply little Fermi surface area and hence a small density of levels at the Fermi energy.[21,22]

The objective of this paper is to determine the experimental bulk electronic structure of Bi by using angle-resolved photoemission spectroscopy (ARPES) coupled with synchrotron radiation and to compare the results with band-structure calculations, assuming strict momentum and energy conservation in the excitation process. Since we are mainly working in normal emission our results will be restricted at present to the ΓT direction of the BZ (see Fig. 1).

The experimental methods are described in Sec. II and the results and discussion of the bulk and surface electronic structure of Bi(111) are presented in Sec. III.

II. EXPERIMENT

The photoemission spectra (PES) were measured at the ''Laboratoire pour l'Utilisation du Rayonnement Electromagnétique'' at the Université de Paris-Sud (Orsay).

The monochromatized storage-ring radiation from either a toroidal-grating or a normal-incidence monochromator served as a light source. The measurements were performed with the light beam set at an angle of incidence of $67°30'$. The resolved electron distribution curves were recorded by using a spherical photoelectron spectrometer with an angular acceptance of $\pm 0.7°$. The spectra were obtained at normal incidence for photon energies between 7.5 and 100 eV with an overall energy resolution smaller than 250 meV for photon energies below 40 eV, and ranging from 250 to 400 meV for photon energy between 40 and 100 eV. Photoemission spectra were in general measured at low temperature ($T \leqslant 20$ K), except for the spectra between 7.5 and 28 eV, which were taken at 300 K.

The Bi(111) samples were single crystal cleaved at low temperature in order to obtain mirrorlike surfaces either *in situ* for photon energy between 60 and 100 eV, or in air prior to mounting in the vacuum chamber for photon energy between 37.5 and 57.5 eV. In the latter case the samples were subsequently cleaned by cycles of argon sputtering (300 V) and annealing (150 °C). The surface cleanliness was then checked by Auger spectroscopy and its crystallinity and orientation by low-energy electron diffraction (LEED). A very intense diffraction pattern with sixfold symmetry was observed in LEED. In Bi the (111) surface does not reconstruct, and the analysis is, therefore, simplified. The results reported in this work were mainly obtained using the second procedure for the sample preparation. The measurements between 37.5 and 100 eV were performed at low temperature in order to minimize the phonon-assisted contributions to the photoemission spectra, because of the low Debye temperature of Bi (120 K).[21] The low-temperature measurements were obtained with the use of a He-flow cryostat working at variable temperatures below 450 K, with a base pressure in the chamber in the low 10^{-10}-mbar range.

III. PHOTOEMISSION RESULTS AND DISCUSSION OF THE ELECTRONIC STRUCTURE

Normal photoemission spectra measured at low temperature, for photon energy between 37.5 and 57.5 eV, and 60 and 100 eV are shown in Fig. 2. By varying the photon energy, the electronic states along the ΓT symmetry line of the bulk Brillouin zone are sampled.[12,16] Two groups of fea-

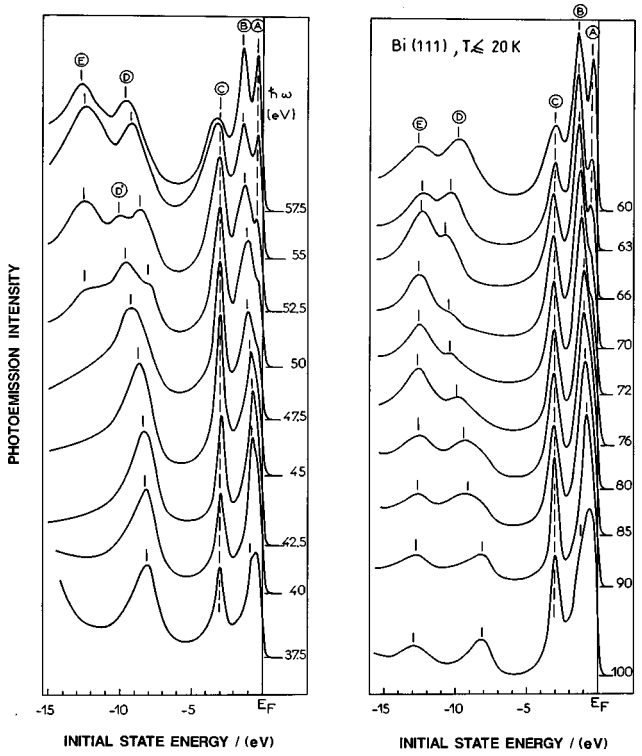

FIG. 2. Normal emission photoelectron spectra measured on the Bi(111) crystal surface at low temperature ($T \leqslant 20$ K). Spectra between 37.5 and 57.5 eV measure photoemission from a surface prepared by ionic bombardment and heated, while the data between 60 and 100 eV are due to emission from a crystal cleaved in ultravacuum at 20 K. Capital letters $A-E$ indicate the main photoemission peaks observed at varying photon energy.

tures are observed: a group of bands (D,D',E), at binding energy larger than 8 eV, which shows rather broad structures (half-width about 2–2.5 eV), corresponding to electron emission from the valence s bands, and structures (A,B,C) originating from the valence p bands, which are near the Fermi level (E_F). The mean splitting between (D,D',E) and peaks (A,B,C) is approximately 10 eV along ΓT.

Let us notice that only structures B, D, D', and E exhibit significant energy dispersion and can be immediately identified as due to the photoemission from occupied bulk bands of Bi. On the other hand, structures A and C, which do not disperse in the observed energy range, are of more difficult interpretation, since they may be due either to nondirect transitions or surface-state emission. Besides, these peaks are narrower than those due to bulk transitions. For bulk transitions the photoemission bandwidth is mostly generated by the momentum broadening $(\Delta k_\perp)$ due to the finite mean free path of the photoelectron.[23–25]

It is well known that angle-resolved photoemission, as measured here, does not uniquely determine both the energy and the perpendicular component of the crystal momentum of the electron $(k_\perp)$, and that some assumptions about the unoccupied final bands are necessary in order to determine the occupied initial bands, i.e., E_i versus $k_{i\perp}$. In order to use standard band mapping methods, one in general reports the dispersion of the initial-state energy versus the final-state energy (see Fig. 3). This plot is most useful in order to select the final-state band and know the experimental energy values (binding energies) of the high-symmetry points Γ and T. For example, it indicates by simple inspection that structures B and D originate from a photoexcitation process, whose matrix elements connect the initial p and s states to the same final-state band and, moreover, that points Γ and T are related to the final-state energies at 40.5 ± 0.5 and 88.0 ± 0.2 eV for the Γ point, and 56.5 ± 0.5 eV for the T point, respectively. Within the free-electron model, the final-state dispersion is described by the relation

$$E_f = \frac{\hbar^2}{2m^*}(k_{f_\perp} - Guuu)^2 + V_0, \tag{1}$$

where V_0 is the bottom of the parabola, measured from E_F, and $k_{f\perp}$ $(=k_{i\perp})$ is the wave vector inside the solid. G_{uuu} is the reciprocal lattice vector, multiple of the smallest vector G_{111} (without umklapp process) and m^* is the effective electron mass (quasielectron mass). By taking $V_0 = -12.8$ eV, corresponding to the lowest-energy value of the first s band, $m^* = 0.88$ m and $G_{uuu} = G_{333}$, one can calculate the final-state energy values of the points T and Γ as 56.5

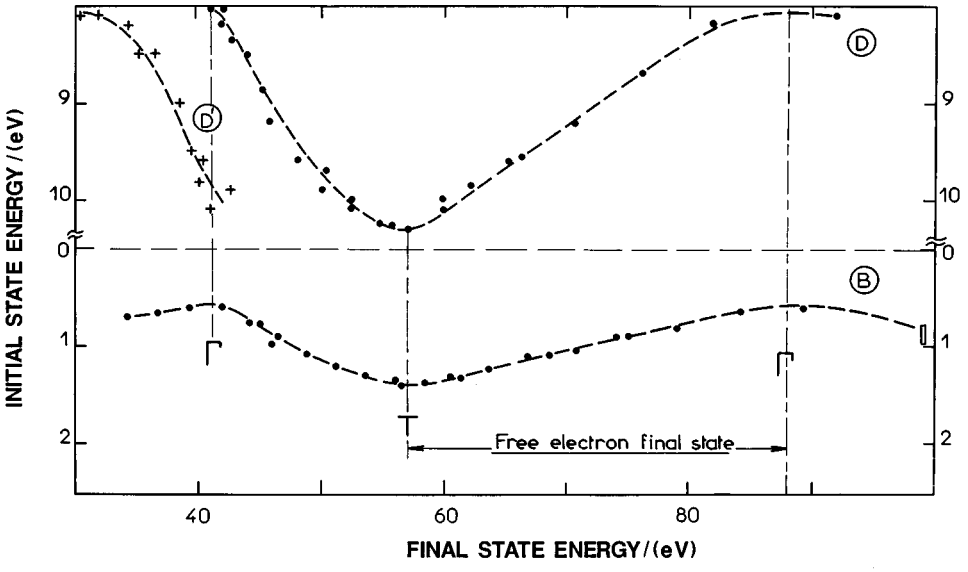

FIG. 3. Initial-state vs final-state energy plot for the experimental bands B,D,D' along the $\Gamma T\Gamma$ symmetry line. The structures B and D originate from photoemission involving the same final state (free-electron parabola).

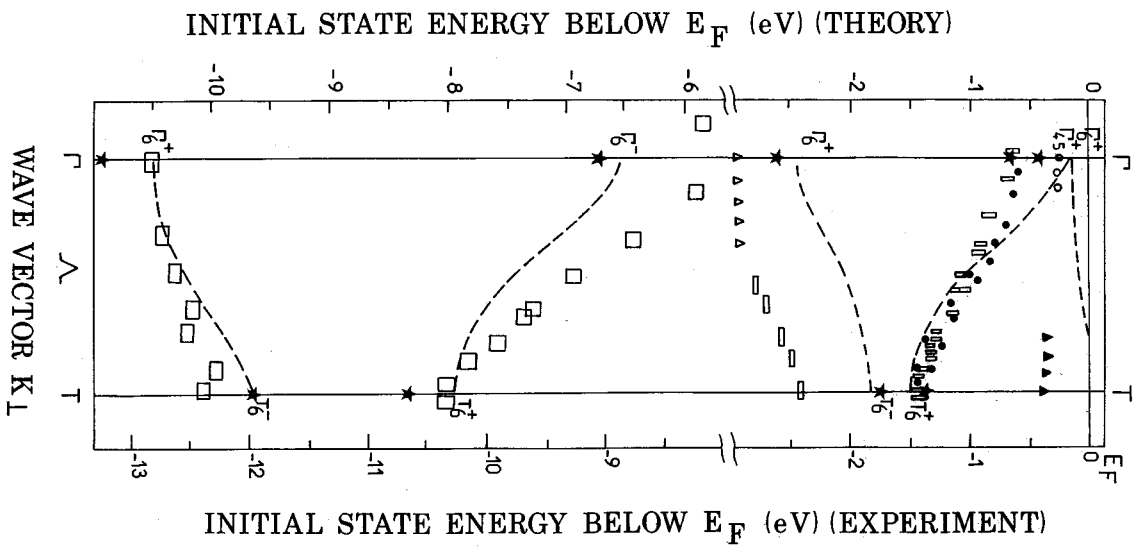

FIG. 4. Valence-band dispersion $E(k_\perp)$ of Bi along the ΓT line. Circles, squares, triangles, and rectangles are experimental points obtained from normal emission spectra in various experimental conditions. The left-hand scale refers to Golin's results only. The symmetry characters of the band and critical points are indicated. The three uppermost bands (binding energy between 0.2 and 2.95 eV at Γ) are of p-like symmetry and the two lower bands are of s-like symmetry. Nondispersing triangles near the Γ point and near the T point (binding energy 2.95 and 0.40 eV, respectively), indicate processes related to the sample surface.

and 88 eV, in good agreement with the values observed experimentally. On the other hand, if we consider the final band dispersion between 40 eV (point Γ) and 56.5 eV (point T) for the structures B and D strong deviations from the free-electron behavior are found. The knowledge of the Bloch final-state dispersion is then used within the direct-transition model in order to plot the experimental E versus k relations. By means of final-state dispersion curve $E_f(k_{f\perp})$ one finds $k_{i\perp}$ $(=k_{f\perp})$, recalling that

$$\mathbf{k}_{f\perp}=\mathbf{K}_{f\perp}-\mathbf{G}_\perp , \tag{2}$$

and also obtains a set of points $E_i(k_{i\perp})$ by the correlated variation of the experimental parameters $\hbar\omega$ and E_i. It is, of course, assumed that $k_f=k_i$ (vertical transitions), i.e., that the crystal momentum is conserved in the photoemission process, if the mean free path $(1/\Delta k_\perp)$ is sufficiently long.[23]

Equation (2) is just the definition for folding an extended zone state $\mathbf{K}_f$ back into the reduced-zone scheme, i.e., relation (1).

The experimental valence bands of Bi, together with the dispersion curves calculated by Golin[12] and the binding-energy values at the symmetry points Γ and T given by Ferreira[13] are shown in Fig. 4, where we have effected a scaling between Golin's calculated curves and measured binding energies below 3 eV, so that the difference between theory and experiment can be estimated by sight. Since the experimental dispersion of the structure B (second p band) is relatively weak, the correction of the peak position due to the relaxation of the k-conservation rule in the photoemission process has been neglected for this band. The structure D (upper s band), however, presents a stronger dispersion, and this is used to evaluate the dispersion of the final state between 41 and 56.5 eV above E_F. This allows us, in turn, to get more experimental points for the higher s band and the second p band (black circles in Fig. 4).

The spectra measured in the high-energy range show a negligible dispersion for the structure with binding energy at Γ of 2.95 eV. However, the dispersion of the third p band can be deduced from a set of measurements carried out at low photon energy ($7.5<\hbar\omega<28$ eV) at room temperature (see Fig. 5). The photoemission features present now a more complex behavior: besides the nondispersing structure C, a new structure C' appears corresponding to the lower p band, which disperses between 2.9 eV ($\hbar\omega=28$ eV) and 2.3 eV [($\hbar\omega=16$ eV) (high-symmetry point T_6^-)].

At lower energy ($\hbar\omega<9$ eV), where the structure B (second p band) shifts towards the Γ point, a relatively narrow A' structure, separated from the nondispersive A peak by approximately 150 meV, occurs in the vicinity of the Fermi level. This structure has been attributed to the uppermost p band near the point Γ. This result is, however, somewhat approximate because of the low instrumental resolution in measuring this binding energy. A different discourse is required for the nondispersive structure A (at about 0.40 eV below E_F), which is also observed in the photon energy range 52.5–67 eV, and is eventually assigned to surface-state emission.

In Table I we have listed the experimental binding energies at the Γ and T symmetry points and compared the measured bandwidths and band gaps with the theoretical band-structure results.

Although the results by Mase[9] and Ferreira[13] have been also considered in the analysis of PES data, we have, however, taken as a basis for discussion the EPM band scheme calculated by Golin together with the APW calculated energies (asterisks) at the symmetry point Γ and T (Fig. 4).

Golin has employed the pseudopotential approach in the form used by Lin and Kleinman for lead salts.[26] The pseudopotential V is formed by a few convenient parameters, which can be adjusted until the resulting band structure agrees with

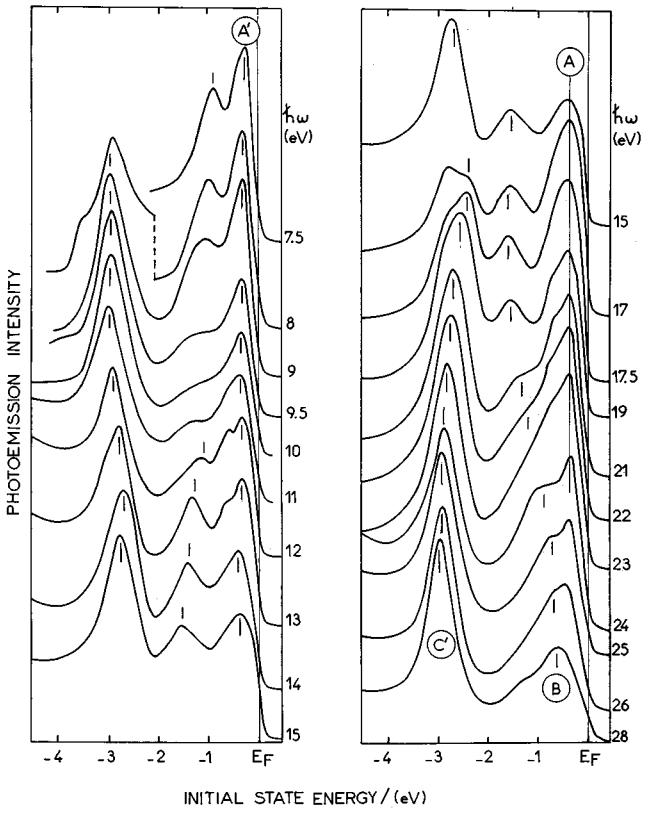

FIG. 5. Room-temperature normal photoemission spectra measured on the Bi(111) surface between 7.5 and 28 eV. The data were taken on a surface prepared by ionic bombardment and annealing.

experiment. It consists of three distinct parts: $V_{\rm loc}$, a local potential that is the dominant term; V_s, an l-dependent term that increases the energies of the levels with s-atomic character, and $V_{\rm so}$, a term representing the spin-orbit coupling. With this pseudopotential, the band structure along symmetry lines and planes of the BZ is calculated (see Fig. 2 of Ref. 12) and the effective masses of the carriers are determined. Golin's calculation is in good quantitative agreement with optical data[7] and qualitative agreement with the effective masses. In bismuth the holes are near the point T_{45}^- as suggested both by theory[9,12] and experiment (g-factor measurements): the quadratic masses and g factors of this level (T_{45}^-) are compared with experiment in Table V of Ref. 12: the uncertainty is mainly due to momentum-matrix elements and many-body effects. Even by varying many parameters, a better agreement with experimental effective masses was not found in the calculations.

In our case, a difference in binding energy is found when we compare the photoemission data with the calculated energies of the lowest p band (Λ_6):a difference of 500 meV is observed between the experimental points and the calculations in Fig. 4. By adjusting the term $V_{\rm so}$, one opens and shifts the two levels Λ_6, so that by a variation of the spin-orbit parameter λ one could lower the theoretical lowest p band (Λ_6) and improve the agreement with the experimental curve.

Also, the uppermost Γ_6^+ and Γ_{45}^+ levels are quasidegenerate and their binding energies are inverted with respect to the experimental points. In addition, the second p band has a theoretical bandwidth that is too large when compared to experiment (0.90 eV).

Figure 4 also shows that a downward scaling of about 2.3 eV is necessary for the band s. The discrepancy is probably due to the Darwin and mass-velocity terms, similarly to what was found in the case of As and Pb.

The agreement seems to be improving, when we consider the APW band calculation made by Ferreira:[13] the upper s band presents, in fact, the correct bandwidth, although a difference in the band dispersion is noticed; it should also be shifted downward by about 0.6 eV at the Γ point (see also Table I). However, for the lowest s band we see that the band center is in agreement with the experiment, although the overall width is too large (1.3 versus 0.6 eV). It should, however, be recalled that in this case the experimental conditions (ionic bombardment) do not permit a high accuracy in the measurement.

Also, we observe for the lowest p band the same discrepancy as in Golin's band scheme: a downward shift of about 0.5 eV is needed to match the experimental points, but a fine

TABLE I. Binding energies (eV) of bismuth at high symmetry points Γ and T of the Brillouin zone. Bandwidths and band gaps observed in photoemission are compared to Golin's and Ferreira's band-structure calculations.

	Γ_6^+	Γ_6^-	Γ_6^+	Γ_6^+	Γ_{45}^-	T_6^-	T_6^+	T_6^-	T_6^+
Golin	−10.47	−6.50	−2.40	−0.147	−0.152	−9.65	−7.9	−1.85	−1.55
Ferreira	−13.20	−9.0	−2.63	−0.66	−0.43	−11.9	−10.6	−1.78	−1.40
Experiment	−12.8	−8.1	−2.9	−0.6	−0.25	−12.2	−10.3	−2.30	−1.50(5)

Bandwidths	s band (1)	s band (2)	p band (1)	p band (2)
Golin	0.8	1.4	0.55	1.4
Ferreira	1.3	1.6	0.85	0.75
Experiment	0.6	2.2	0.60	0.90
Gaps	$T_6^-T_6^+$	$\Gamma_6^-\Gamma_6^+$	$T_6^-T_6^+$	$\Gamma_6^+\Gamma_{45}^+$
Golin	1.75	3.9	0.3	−0.005
Ferreira	1.3	6.35	0.38	+0.23
Experiment	1.9	5.25	0.85	~0.4

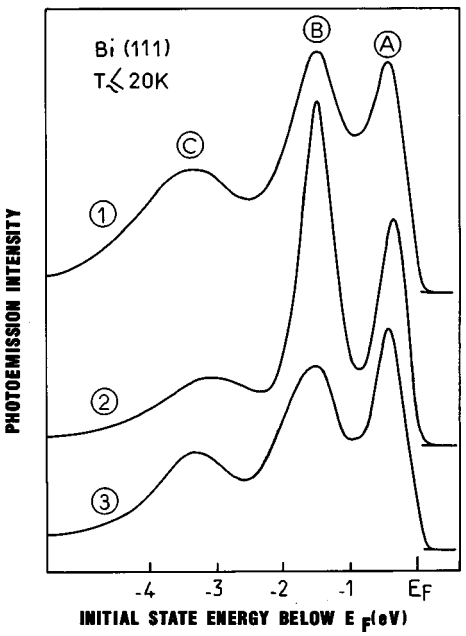

FIG. 6. Effect produced by the surface roughness on the photoemission feature C. Photoemission spectra measured at photon energy $\hbar\omega=57.5$ eV at $T\leqslant 20$ K on the surface prepared by ionic bombardment (sample 1) or cleaved in vacuum (samples 2 and 3) are compared. Note that spectra 1 and 2 are taken at normal emission ($\theta=0$), while spectrum 3 is obtained at off-normal emission with $\theta=1.5°$.

agreement with experiment is found for the second p band, both for the bandwidth and the location and level order of the symmetry points Γ_6^+ and Γ_{45}^+.

Let us now discuss the peaks A (at 0.40 eV) and C (2.95 eV), which do not present dispersion with $k_\perp$ over the major part of the ΓT line. In addition to bulk dispersing transitions, there are two more types of peaks commonly observed in valence-band photoemission spectra: surface states and surface resonances. Both are due to additional one-electron states near the surface of the crystal, but surface states are by definition restricted to bulk band gaps and do not disperse with $k_\perp$, while surface resonances may not be in energy gaps and may hybridize with bulk levels, thus having larger half-widths.

The narrow peak A is observed in the low-temperature spectra between 52.5 and 66 eV, near point T, while the peak C is observed between 37.5 and 100 eV and is rather sharp around 45 and 90 eV. This peak C is thus observed in Fig. 2 in the whole energy range and presents an oscillatory behavior of the photoemission intensity which has its maxima at $\hbar\omega=45$ and 90 eV, where the final state reaches the Γ point around 42 and 87 eV (see Fig. 3). These oscillations of the photoelectric cross section have been first observed for surface states on the Cu(111) surface.[27] However, this peak broadens and presents a small dispersion in the vicinity of point T, indicating bulk photoemission. In order to clarify the nature of the peaks, new photoemission measurements are required.

Figure 6 compares the photoemission spectra measured at $\hbar\omega=57.5$ eV on samples of Bi subjected to ionic bombardment (spectrum 1) and cleaved in vacuum (spectra 2 and 3). We see a reduction in the intensity of band C for sample 2 cleaved in vacuum and a corresponding increase of the bulk feature, B with respect to the C and A structures. If we repeat the same measurements at the emission angle $\theta=1.5°$ off normal on the cleaved surface, we note that the intensity ratio is inverted, i.e., the bulk structure B is reduced in strength with respect to the ''surface'' structures. Also, the effect strengthens when we increase the off-normal emission angle θ. The obtained result is explained by saying that the bombarded surface integrates the emission intensity for some values of the polar angle θ: the surface due to ionic bombardment is no more smooth and the consequent surface roughness causes a $k_\parallel$ integration ($\Delta k_\parallel$) at the crystal surface. Any smearing in k resolution, either experimentally (analyzer collection angle) or physically (surface roughness), results in a measurement that is averaged over a region of the k space.

We finally consider the sharp dispersionless structure A observed at normal emission near point T, at 0.40 eV below E_F. This structure, obtained in the spectra measured at low and high photon energy, does not move with $\hbar\omega$, and is located near T, where band-structure calculations and various experimental results agree to locate the holes in semimetal Bi. A straightforward hypothesis would assign this feature to a surface state in the Γ_{45}^+-Γ_6^+ gap, that is to band-gap or surface emission. This possibility has been tested experimentally, by means of a study of this structure as a function of the temperature and exposition to an oxygen atmosphere.[28] In order to better characterize this emission, the energy dispersion parallel to the surface was also measured and compared to the calculated energy dispersion. The good agreement between theory and experiment indicated that a correct characterization of the surface state was obtained.[28]

The presence of surface (and bulk) states in the range of the binding energies (between E_F and 4 eV) of the p-like valence bands of Bi(111) is also confirmed by the analysis of ARUPS measurements recently carried out in order to study the dispersion of the p-like valence bands along and perpendicular to the ΓT direction of the BZ. These preliminary experimental results,[29] which are now being analyzed, shows four dispersing peaks (versus $k_\parallel$) that seem to confirm the interpretation presented here.

IV. CONCLUSIONS

Accurate valence-band dispersion $E(\mathbf{k})$ along the symmetry direction Γ-Λ-T has been determined for semimetallic Bi using ARPES with synchrotron radiation. At these photon energies ($7\leqslant h\nu\leqslant 100$ eV), bulk emission features can be described within the direct transition-model and free-electron-like final-state dispersion above 58 eV. Some emission is due to dispersionless features and has been attributed to photoemission from the surface.

Experimental valence dispersions and critical-point energies are also compared with EPM and APW band-structure calculations. We have found that both calculations fail to estimate the s- and p-state bandwidth and the critical-point binding energies with accuracy, specially for the lower s bands. However, the two calculations show a different discrepancy in their description of the band structure of Bi.

In the EPM calculations, a downward scaling by about 2.3 eV is needed for the *s* bands in order to match the experimental curves; the width of the second *p* band is overestimated and, close to the Fermi level, the Γ_6^+ and Γ_{45}^+ points are inverted. The APW calculations give results in much better agreement with the experiments, both for the *s* and *p* bands. In this latter case, the Γ_6^+ and Γ_{45}^+ points are in the right order and the bandwidths are correctly described. A downward shift of about 0.5 eV for the lowest *p* band is, however, required, as in the EPM calculation, in order to fit the experimental curves. In conclusion, it seems that, on the grounds of the new experimental results here reported, a new *ab initio* band-structure calculation of the semimetallic bismuth would be of great interest and is called for.

*Also at: Laboratoire pour l'Utilisation du Rayonnement Electromagnétique (LURE), Université Paris-Sud, F-91405 Orsay CEDEX, France.

[1] M. H. Cohen and E. I. Blount, Philos. Mag. **5**, 115 (1960).
[2] B. Lax, J. G. Mavroides, H. J. Leiger, and R. J. Keyes, Phys. Rev. Lett. **4**, 241 (1960); R. N. Brown, J. G. Mavroides, and B. Lax, Phys. Rev. **129**, 2055 (1961).
[3] M. H. Cohen, Phys. Rev. **121**, 387 (1961).
[4] R. N. Bhargava, Phys. Rev. **156**, 785 (1967).
[5] G. E. Smith, G. A. Baraff, and J. M. Rowell, Phys. Rev. **135**, A1118 (1964).
[6] B. Mc Combe and G. Seidel, Phys. Rev. **155**, 633 (1967).
[7] M. Cardona and D. L. Greenway, Phys. Rev. **133**, A1685 (1964).
[8] A. L. Jain and R. Jaggi, Phys. Rev. **135**, A708 (1964).
[9] S. Mase, J. Phys. Soc. Jpn. **13**, 434 (1958); **14**, 584 (1959).
[10] A. A. Abrikosov and L. A. Falkovski, Zh. Eksp. Teor. Fiz. **43**, 1089 (1962) [Sov. Phys. JETP **16**, 769 (1963)].
[11] L. A. Falkovskii and G. S. Razina, Zh. Eksp. Teor. Fiz. **49**, 265 (1965) [Sov. Phys. JETP **22**, 187 (1966)].
[12] S. Golin, Phys. Rev. **166**, 643 (1968).
[13] L. G. Ferreira, J. Phys. Chem. Solids **28**, 1891 (1967); **29**, 357 (1968).
[14] P. J. Lin and L. M. Falicov, Phys. Rev. **142**, 441 (1966).
[15] L. M. Falicov and P. J. Lin, Phys. Rev. **141**, 562 (1965).
[16] L. M. Falicov and S. Golin, Phys. Rev. **137**, A871 (1965).
[17] S. Golin, Phys. Rev. **140**, A993 (1965).
[18] L. Ley, R. A. Pollack, S. P. Kowalczyk, R. McFeely, and D. A. Shirley, Phys. Rev. B **8**, 641 (1973); L. Ley, R. A. Pollack, S. Kowalczyk, and D. A. Shirley, Phys. Lett. **41A**, 429 (1972).
[19] D. Liebowitz, J. Muratore, Y. H. Kao, and N. J. Shevchik, Solid State Commun. **22**, 759 (1977).
[20] R. W. G. Wyckoff, *Crystal Structures* (Interscience, New York, 1960), Vol. 1.
[21] C. Kittel, *Introduction to Solid State Physics*, 4th ed. (Wiley, New York, 1971).
[22] N. W. Ashcroft and N. D. Mermin, *Solid State Physics* (Holt, Rinehart, and Winston, New York, 1976).
[23] P. J. Feibelman and D. E. Eastman, Phys. Rev. B **10**, 4932 (1974).
[24] P. Thiry, D. Chanderis, J. Lecante, C. Guillot, R. Pinchaux, and Y. Petroff, Phys. Rev. Lett. **43**, 82 (1979).
[25] G. Jezequel and I. Pollini, Phys. Rev. B **41**, 1327 (1990).
[26] P. J. Lin and L. Kleinman, Phys. Rev. **142**, 478 (1966).
[27] S. G. Louie, P. Thiry, R. Pinchaux, Y. Petroff, D. Chanderis, and J. Lecante, Phys. Rev. Lett. **44**, 549 (1980).
[28] G. Jezequel, Y. Petroff, R. Pinchaux, and F. Yndurain, Phys. Rev. B **33**, 4352 (1986).
[29] J. Thomas, G. Jezequel, and I. Pollini (unpublished).